

## Table of Contents

1	Introduction .....	2
2	Procedure to obtain the center of the contrast target .....	2
2.1	Extract regions of interest of each target.....	3
2.2	Calculate an approximate 3D center of the image using 2D imaging methods ....	3
2.3	Calculate a refined center of the image using dimensional and intensity data .....	4
3	Test methodology .....	6
3.1	Test setup.....	6
3.2	Summary and discussion of the results .....	7
4	Conclusion .....	8
5	References .....	8

# METHOD TO DETERMINE THE CENTER OF CONTRAST TARGETS FROM TERRESTRIAL LASER SCANNER DATA

Prem Rachakonda\*, Bala Muralikrishnan\*, Daniel Sawyer\*, Ling Wang\*\*

\*Dimensional Metrology Group,  
Engineering Physics Division  
National Institute of Standards and Technology,  
Gaithersburg, MD, USA

\*\*Department of Automation, School of  
Mechanical and Electrical Engineering,  
China Jiliang University, Hangzhou,  
Zhejiang Province, 310018, P. R. China

## 1 INTRODUCTION

Terrestrial laser scanners (TLSs) are instruments that can measure 3D coordinates of objects at high speed using a laser, resulting in high density 3D point cloud data. Contrast targets are some of the most common targets used with TLSs to establish a scale or register multiple scan datasets. These targets are also known as checkerboard targets or signalized targets and their design provides a way to calculate their geometric center by using intensity data along with the dimensional data. Large contrast targets are needed when scanning at longer distances; however, unlike other geometric targets such as spheres, fabrication of large contrast targets is relatively inexpensive. Even though contrast targets are used with TLSs, the algorithms to calculate their centers are proprietary and/or work only with proprietary data formats.

In this context, this paper provides a novel method that was developed at the National Institute of Standards and Technology (NIST) to calculate the derived point or the center of a contrast target (henceforth termed as CCT) and compares its performance with commercial software, in various scan conditions.

## 2 PROCEDURE TO OBTAIN THE CENTER OF THE CONTRAST TARGET

Calculating the center of a contrast target has not been studied extensively in open literature. This paper describes one method to obtain the center of a contrast target which involves multiple steps, where each successive step attempts to refine the center of the target obtained in the previous step. For the target depicted in Figure 1, the center is the location where the two black squares meet.

Most software that are provided by TLS manufacturers output intensity or color data along with dimensional data for their scans. For this procedure, the dimensional data was exported along with intensity data (XYZI format). Some TLSs provide dimensional data along with color intensity (XYZRGB). Here, X, Y, Z correspond to the dimensional data, I is the intensity data and R, G, B correspond to red, green, blue channel intensity data. If the data obtained is in the form of XYZRGB, the RGB data needs to be converted to intensity values using a weighted sum using the formula  $I = 0.299 \times R + 0.587 \times G + 0.114 \times B$  [1]. Subsequently, the XYZI formatted data can be processed using the following steps to obtain the center of a contrast target.

1. Extract the data corresponding to the region of interest of the contrast target within the scene.
2. Calculate an approximate 3D location of the center of the target using 2D imaging methods.

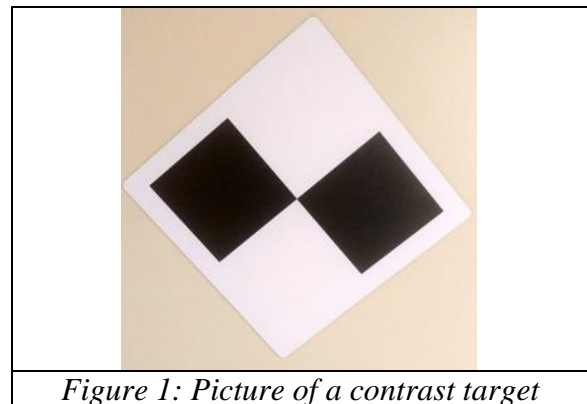
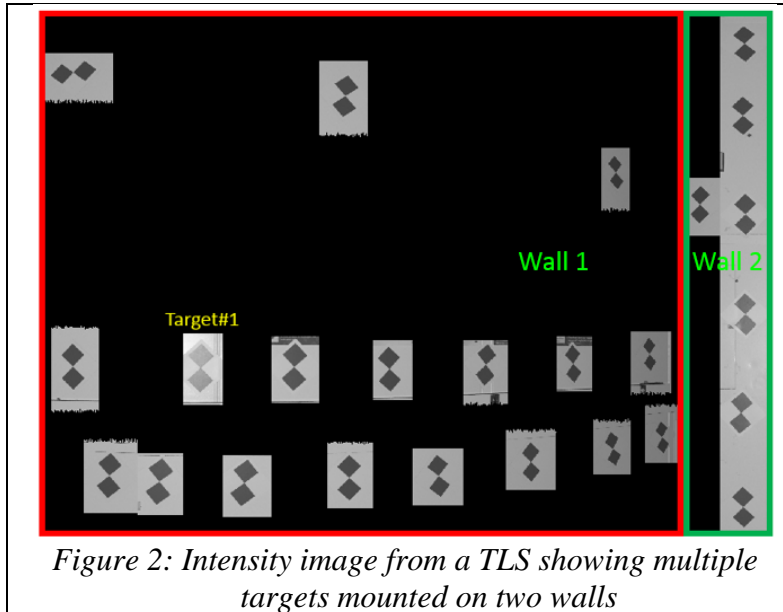


*Figure 1: Picture of a contrast target*

3. Obtain a refined location of the center of the target using dimensional and intensity data.

### 2.1 Extract targets' regions of interest

The first step in this process was to extract the regions of interest from a scan. This step



lowers the complexity and number of computations needed to find the 2D center of the target. Figure 2 is the extracted intensity image of a scan which shows multiple checkboard targets placed around a room in different orientations. Data corresponding to individual targets need to be cropped/separated. This process needs to be performed for both the dimensional and the intensity data.

This cropping of the data (XYZI) can be done either manually or automatically. The manual method may use any point cloud manipulating software for

cropping, whereas the automatic methods may use a template matching method. For this work, all the regions of interest were cropped manually once for the first dataset and the same cropping regions were used to crop the remaining datasets. All subsequent processing described next was performed using automated methods.

### 2.2 Calculate the target's approximate 3D center using 2D imaging methods

To obtain the center of the target, the intensity information can be used to generate a 2D image of the target. Subsequently, this image is processed using edge detection methods along with the Hough transform [2]. These methods aid in detecting the intersecting lines in a checkerboard-like pattern [3]. The Hough transform is a mature algorithm and is built into software like MATLAB\* which was used to process this data. As is usual with many image processing algorithms some level of adjustments is required when the nature of the image changes (low contrast, high noise etc.). The steps to extract an approximate target center (CCT) are as follows:

- i. Each cropped XYZI dataset was processed and an image was generated to show a single contrast target as shown in *Figure 3a*.
- ii. The image generated by the previous step was cropped further using a circular mask to display the central region where the two black squares touch each other. Care must be taken to avoid any other regions with intersecting lines/corners as shown in *Figure 3b*. The masking was done automatically using a predefined mask position and size. Using a square mask instead of a circular mask would lead to detection of additional lines that are at the edges of the square mask.

---

\* Disclaimer: Commercial equipment and materials may be identified in order to adequately specify certain procedures. In no case does such identification imply recommendation or endorsement by the National Institute of Standards and Technology, nor does it imply that the materials or equipment identified are necessarily the best available for the purpose.

- iii. Lines/edges were emphasized in masked image using a “Canny edge” algorithm.
- iv. A Hough transform was performed on the image from the previous step and the intersecting lines are obtained. It is possible that there may be more than two lines due to the nature of the image (unclean targets, uneven target plane, shadows etc.). Care must be taken to apply appropriate filters to obtain only two intersecting lines at the center of the target.
- v. The two lines obtained in the previous step were intersected to obtain a 2D approximation of the center of the contrast target  $CCT_1$  as shown in *Figure 3c*.

In the event of failure of the 2D method described above, a manual method may be used to pick the approximate 2D center from the image. It should be noted that  $CCT_1$  was obtained from image data in units of pixels. Even though the pixels are integer numbers,  $CCT_1$  may not have integer values.

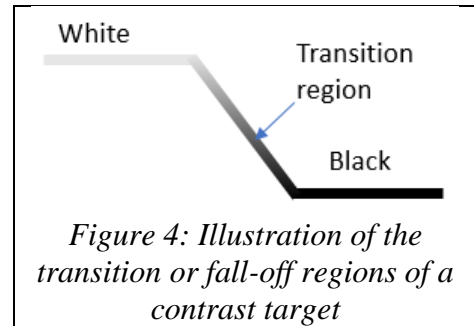
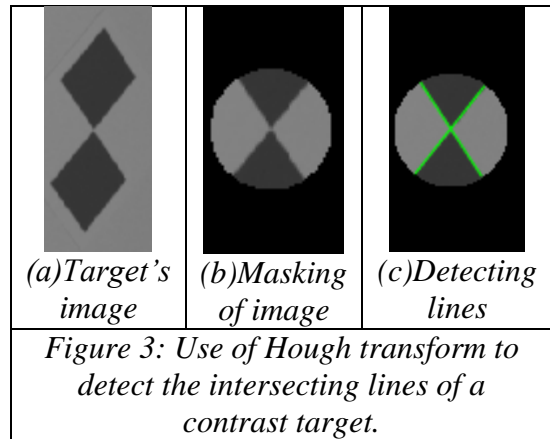
Each pixel in the 2D image has a corresponding 3D coordinate and an intensity value. To obtain an approximate 3D center, the pixel center coordinates  $CCT_1$  are rounded and an integer pixel location  $CCT_2$  closest to the  $CCT_1$  was obtained. This modified pixel location has a corresponding 3D coordinate  $X_3, Y_3, Z_3$  and intensity value  $I_3$ . The 3D coordinate corresponding to  $CCT_2$  was then  $CCT_3 = (X_3, Y_3, Z_3)$ .

### 2.3 Calculate a refined target center using dimensional and intensity data

One method to calculate the 3D center of the contrast target was described in the previous subsection. When multiple scans of the same target were processed, the approximate 3D coordinates of the centers ( $CCT_3$ ) were found to have poor repeatability ( $1\sigma > 1$  mm), much larger than the expected repeatability of the system and the setup. To improve the calculation of target centers, a new method was conceived which uses intensity data along with dimensional data in non-radial directions. To perform this, first the 3D data in Cartesian coordinate system was converted to data in a spherical coordinate system of form  $(H, V, R)$ , where  $H$  is the horizontal/azimuth angle,  $V$  is the vertical/elevation angle and  $R$  is the radial distance to each measured point.

A new dataset was created that was comprised of the angles  $H, V$  and the intensity data  $I$ . Henceforth, this will be referred as the HVI domain in this paper. The radial data ( $R$ ) was ignored at this point. To improve the results, the following modifications were performed on the data:

1. The density of data in the HVI domain was increased to 300 times the original point density by interpolation using a cubic polynomial. This was found to lower the uncertainty in calculating the intersection point. Although cubic polynomial interpolation has a possibility of wild swings in the interpolated points, the data was visually inspected after interpolation to ensure that such issues do not exist in the region of interest (fall-off region in *Figure 4*). Other



interpolation techniques were also explored, however cubic interpolation was observed to perform adequately for most datasets.

2. In an ideal scan of a contrast target, the intensity data typically has a minimum value of 0 (black) and maximum value of 1 (white). However, most scans of contrast targets don't have such values for their black and white regions. For example, the intensity may range from 0.25 to 0.75. To lower the uncertainty of determining the CCT, intensity data was normalized/scaled from 0 to 1.

In the HVI domain, the intensity values corresponding to the intersecting lines in a 2D image have a sharp fall-off as illustrated in Figure 4. In this fall-off region, the intensity drastically changes from  $I \approx 1$  to  $I \approx 0$ . These regions in the HVI domain are shown in Figure 5 where the colored regions in the middle are the high density interpolated points corresponding to the fall-off region. The following steps are then performed to obtain the intersection point:

- a. The fall-off region in the HVI domain was obtained by discarding the surfaces corresponding to extreme intensities (black and white in Figure 5) that are over 0.5 times the standard deviation ( $0.5 \sigma$ ) from the mean intensity value. This value of  $0.5 \sigma$  was empirically determined and it ensured that only data belonging to the intersecting fall-off regions were obtained.
- b. This fall-off region was then split into four parts after truncating the central cylindrical region close to the approximate center. This is performed using an automated method and this truncation enables the intersecting regions to be separated into four parts (as shown by the colored regions in Figure 5).
- c. The intensity data from four datasets in the HVI domain was then discarded, keeping only H and V. This process essentially collapses the data to a single plane in HV domain, yielding datasets corresponding to four lines on the target.
- d. In this step, a 2D intersection point in the HV domain was obtained. This can be obtained in one of three ways:
  - i. The four line datasets can be intersected using a least-squares method in the HV domain to yield the center of the target ( $H_c, V_c$ ).
  - ii. The four line datasets can be grouped together into two datasets corresponding to two lines. These datasets can be least-squares fit to two lines, which can then be intersected to obtain ( $H_c, V_c$ ).
  - iii. Alternatively, before step#c, the four surfaces in the HVI domain (colored regions in Figure 5) can be fit to planes. These four plane equations can be solved using a least-squares method to perform a four-plane intersection. This method results in an intersection point ( $H_c, V_c, I_c$ ) and thereby obtaining a center ( $H_c, V_c$ ) in 2D.

In general, it was found that 2D line intersection of two lines was more repeatable than the other two methods to yield an intersection point ( $H_c, V_c$ ). Both the plane and line fitting routines were performed iteratively after excluding data points whose corresponding

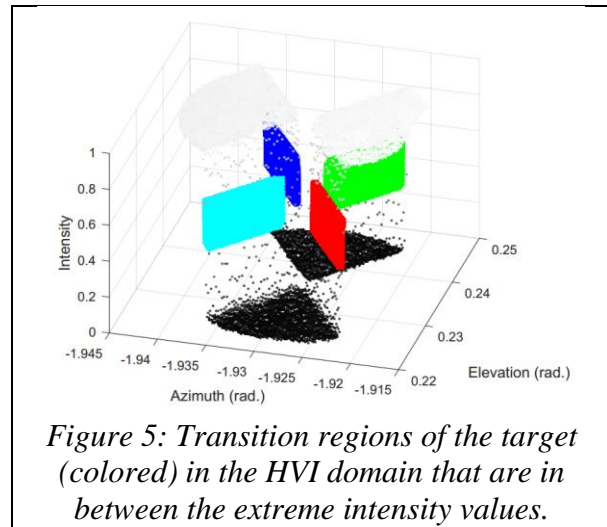


*Figure 5: Transition regions of the target (colored) in the HVI domain that are in between the extreme intensity values.*

residuals exceeded three times the standard deviation of the residuals. The iterations were terminated when there were no more points to exclude.

- e. The radial value of the center ( $R_c$ ) was the radial value of  $CCT_3$  in spherical coordinate system. It should be noted that  $CCT_3$  was calculated using 2D imaging methods described in section 2.2. This value of  $R_c$  is an approximate value and will be improved in the subsequent steps.
- f. The center ( $H_c, V_c, R_c$ ) was then converted to a Cartesian coordinate system to obtain  $CCT_4 = (X_c, Y_c, Z_c)$ .
- g. As a final step,  $CCT_4$  was projected onto the plane of the contrast target in the XYZ domain. This was performed by intersecting the line joining the origin and  $CCT_4$  with the plane of the contrast target. This projected point  $CCT_5 = (X_p, Y_p, Z_p)$  was the final center of the contrast target. This projection method was required to ensure that the final center  $CCT_5$  lies on the plane of the contrast target.

### 3 TEST METHODOLOGY

To understand the currently available methods and to compare them with the method described in this paper, three commercial software packages were used and repeatability studies were conducted. Two contrast targets were scanned 10 times and their CCTs and the standard deviations ( $1\sigma$ ) of those CCTs were calculated using each software. Lower  $1\sigma$  values of all the 3D coordinates ( $\sigma_x, \sigma_y, \sigma_z$ ) indicates a more robust algorithm. This metric however considers only the precision of the centers but not their accuracy. It should be noted that there may be other software which may perform better, but were inaccessible to the authors at the time of writing this paper. One commercial software (Method#1) yielded lowest  $1\sigma$  values (lower by an order of magnitude) and this software was used to compare the method described in this paper (Method#2).

*Table 1: Comparison of the target center parameters*

Target #	Method#1 ( $\mu\text{m}$ )				Method#2 ( $\mu\text{m}$ )				L (m)	M	D	$\theta^\circ$
	$\sigma_{H1}$	$\sigma_{V1}$	$\sigma_{R1}$	$\sigma_{D1}$	$\sigma_{H2}$	$\sigma_{V2}$	$\sigma_{R2}$	$\sigma_{D2}$				
1	48	76	40	53	75	96	34	63	4.4	1.2	1.2	2
2	37	68	29	51	35	76	26	53	4.5	1.0	1.0	11
3	48	71	33	53	47	65	28	47	4.5	0.9	0.9	6
4	54	69	30	53	50	70	27	52	4.5	0.9	1.0	6
5	57	80	27	59	50	80	24	57	4.7	0.9	1.0	15
6	48	72	36	47	46	69	30	46	4.7	0.9	1.0	16
7	35	67	28	37	35	64	27	41	4.7	1.0	1.1	19
8	42	85	36	62	41	82	34	62	4.8	1.0	1.0	22
9	16	86	28	55	12	81	25	53	4.9	0.9	1.0	15
10	8	64	24	34	14	63	23	34	5.0	1.2	1.0	18
11	60	87	32	72	57	86	28	69	5.0	0.9	1.0	26
12	39	111	21	72	46	118	25	76	5.1	1.1	1.1	5
13	55	123	29	87	55	121	24	84	5.1	0.9	1.0	6
14	38	94	33	67	40	94	30	65	5.2	1.0	1.0	31
15	18	108	22	70	23	107	21	71	5.2	1.1	1.0	5
16	64	124	29	87	66	120	28	85	5.2	1.0	1.0	5
17	13	120	22	75	19	119	19	75	5.4	1.1	1.0	5
18	56	102	34	75	56	100	29	74	5.4	0.9	1.0	34
19	34	129	17	78	20	123	19	76	5.6	0.9	1.0	4
20	24	108	39	71	23	115	30	70	5.7	0.9	1.0	23
21	48	109	34	75	47	107	36	76	5.7	1.0	1.0	39
22	66	115	30	82	61	109	29	80	6.2	1.0	1.0	44
23	25	111	30	69	23	116	26	73	6.3	1.0	1.1	44
24	51	122	31	81	50	119	24	81	6.4	0.9	1.0	47
25	65	120	30	88	63	118	34	85	6.6	1.0	1.0	47

#### 3.1 Test setup

The test setup involved placing 25 contrast targets on two walls as depicted in Figure 2. These targets were square in shape,  $\approx 225$  mm wide, fabricated out of a flexible plastic material and have a magnetic backing for the purposes of mounting. Seven targets were mounted on a wall (green wall) on the right distributed vertically and the rest are mounted on a wall that was perpendicular (red wall), distributed horizontally. Even though these targets appear to be in the same plane in Figure 2 (planar view), they are in fact on two walls that are perpendicular. The TLS

was placed at approximately 5 m from both the walls and the distance to each target (L) and the angles of incidence ( $\theta$ ) are listed in *Table 1*. The angle of incidence  $\theta$  is the angle between the target's surface normal and the laser beam at the target's nominal center.

To perform an evaluation, these targets were scanned 10 times using a TLS. One such scan is depicted in Figure 1. Data acquired by this TLS was exported both to its own proprietary file format and to the XYZI format. Commercial software (Method#1) was used to process the data in this proprietary file format and the CCT of all the targets were obtained. This software did not have the capability to process the data in the XYZI format.

After processing the data, the standard deviation of the centers in spherical coordinates calculated by Method#1 was  $\sigma_1$ , and as calculated by Method#2 was  $\sigma_2$ . Here  $\sigma_1 = (\sigma_{A1}, \sigma_{E1}, \sigma_{R1})$  and  $\sigma_2 = (\sigma_{A2}, \sigma_{E2}, \sigma_{R2})$ . To perform a comparison in the units of length, the standard deviations in azimuth and elevation were multiplied by the average radial distance value of the center. i.e.,  $\sigma_{H1} = R_1 \times \sigma_{A1}$ ,  $\sigma_{V1} = R_1 \times \sigma_{E1}$ ,  $\sigma_{H2} = R_2 \times \sigma_{A2}$ ,  $\sigma_{V2} = R_2 \times \sigma_{E2}$ . Here  $R_1$  and  $R_2$  were the average radial distances of the center as determined by Method#1 and Method#2 respectively. Two other parameters,  $\sigma_{D1}$  and  $\sigma_{D2}$  were calculated, which were the  $1\sigma$  values of the distances of the centers about the mean value of the center calculated by Method#1 and Method#2 respectively. These are listed in *Table 1* along with a parameter  $D = \sigma_{D2}/\sigma_{D1}$ .

Ideally, the corresponding standard deviation values of both the methods ( $\sigma_1$  and  $\sigma_2$ ) should be equal, but they are not. To make the comparison simpler, a quality factor M given by equation 1 was introduced to compare the methods at each CCT and *Table 1* shows all the parameters calculated using both the methods using the 10 repeat measurements. This method of comparison is useful since Method#1 was found to be consistently producing centers with lower variation among the three commercial software packages that were evaluated.

$$M = \frac{M_{AZ} + M_{EL} + M_{RR}}{3} \quad 1$$

$$\text{where, } M_{AZ} = \frac{\sigma_{A2}}{\sigma_{A1}}, M_{EL} = \frac{\sigma_{E2}}{\sigma_{E1}} \text{ and } M_{RR} = \frac{\sigma_{R2}}{\sigma_{R1}}.$$

If the standard deviation values from both the methods are identical,  $M = 1$ . If Method#1 performs better than Method#2 then  $M > 1$  and *vice versa* if  $M < 1$ . There may be cases where  $M = 1$  if Method#1 outperforms in one component and underperforms in another. This metric M gives a good estimate of the overall method performance and  $M_{AZ}$ ,  $M_{EL}$ ,  $M_{RR}$  reveal the performance of the method in individual spherical coordinate components.

### 3.2 Summary and discussion of the results

The centers of the contrast targets were calculated using a method involving multiple steps. The steps described in this paper are summarized below:

- CCT<sub>1</sub>: 2D center using image processing methods
- CCT<sub>2</sub>: 2D center with integer values of CCT<sub>1</sub>
- CCT<sub>3</sub>: 3D center corresponding to CCT<sub>2</sub>
- CCT<sub>4</sub>: 3D center using HVI domain method
- CCT<sub>5</sub>: CCT<sub>4</sub> projected on the target's plane

Two notable trends affected the quality of Method#2. First, it was observed that the value of M

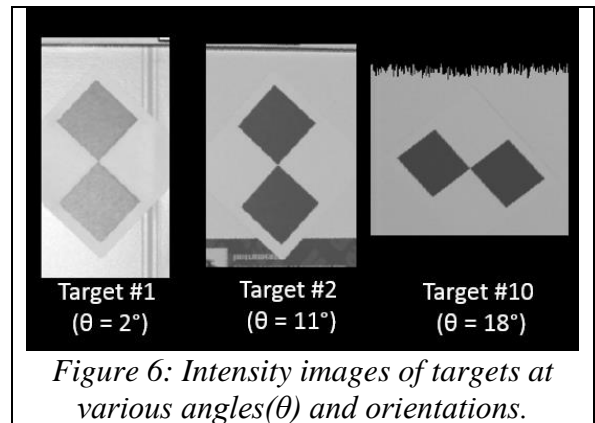


*Figure 6: Intensity images of targets at various angles( $\theta$ ) and orientations.*

was *not* significantly dependent on the angle of incidence ( $\theta$ ), but on the intensity variations in the black and the white regions of the target as shown in Figure 6. Targets that were placed at  $\theta < 7^\circ$  (shallow incidence angles) resulted in high intensity regions in the black part of the target. Second, target #10 also showed higher value of  $M$  as it was oriented differently compared to all the other 24 targets (see Figure 6). However, overall it can be observed from Figure 7b that Method#2 performs reasonably well in all the three components.

The distances between the centers obtained from Method#1 and Method#2 were calculated and the average distance between the centers at all the locations was  $\approx 0.14$  mm. There was no systematic bias that was observed in the azimuth or elevation coordinate differences of centers from both the methods, but there was a bias in the radial direction, an average of  $\approx 0.12$  mm. This bias could be a result of ensuring that the CCT is on the least-squares fitted plane of the target. It should be noted that the accuracy of either method cannot be ascertained using a single point measurement. Such a comparison would require test procedures involving calibrated lengths between two contrast targets in various orientations.

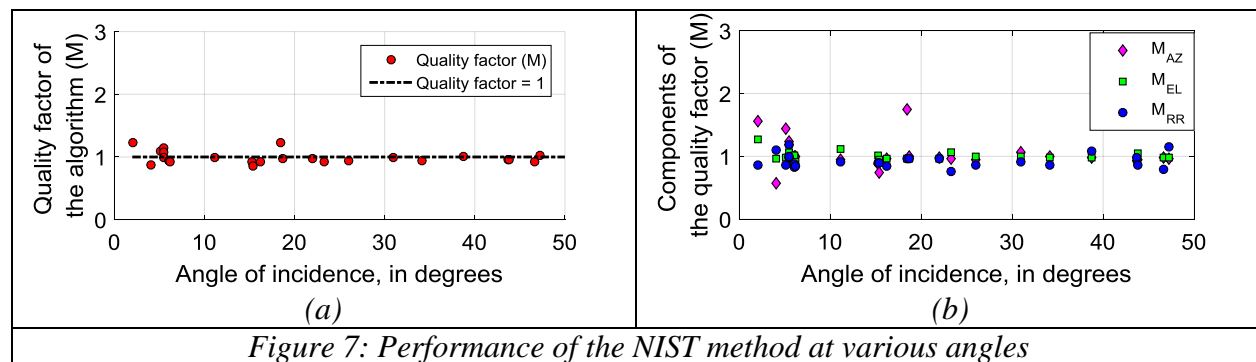


Figure 7: Performance of the NIST method at various angles

#### 4 CONCLUSION

This paper presents a novel method developed at NIST to calculate the center of a contrast target and compares it with the results from other available software. It was observed that the NIST method performs reasonably well for most targets. More work is planned to ascertain the method's performance for various test cases (target orientations, data densities etc.). This is to ensure that the parameters used to deduce the target centers are more robust and applicable for scans with varying data quality.

#### 5 REFERENCES

- [1] ITU-R BT.601-71 - Studio encoding parameters of digital television for standard 4:3 and wide-screen 16:9 aspect ratios [https://www.itu.int/dms\\_pubrec/itu-r/rec/bt/R-REC-BT.601-7-201103-I!!PDF-E.pdf](https://www.itu.int/dms_pubrec/itu-r/rec/bt/R-REC-BT.601-7-201103-I!!PDF-E.pdf) (Retrieved 8/2/2017)
- [2] Duda, R., Hart, P., "Use of Hough Transformation to Detect Lines and Curves in Pictures", Communications of the ACM, January 1972, Vol.15, No. 1
- [3] [http://www.vision.caltech.edu/bouguetj/calib\\_doc/htmls/example.html](http://www.vision.caltech.edu/bouguetj/calib_doc/htmls/example.html) (Retrieved 6/21/2017)